INL/JOU-22-69290-Revision-0

Impact of Lanthanide Complexation and Temperature on the Chemical Reactivity of N,N,N',N'-tetraoctyl diglycolamide (TODGA) with the Dodecane Radical Cation

Gregory P Horne, Jacy Kathleen Conrad, Jeffrey R McLachlan, Brian Rotermund, Andrew Cook, Stephen Mezyk

INL/JOU-22-69290-Revision-0

Impact of Lanthanide Complexation and Temperature on the Chemical Reactivity of N,N,N',N'-tetraoctyl diglycolamide (TODGA) with the Dodecane Radical Cation

Gregory P Horne, Jacy Kathleen Conrad, Jeffrey R McLachlan, Brian Rotermund, Andrew Cook, Stephen Mezyk

September 2022

Idaho National Laboratory
Idaho Falls, Idaho 83415

http://www.inl.gov

Prepared for the
U.S. Department of Energy
Under DOE Idaho Operations Office
Contract DE-AC07-05ID14517

Impact of Lanthanide Complexation and Temperature on the Chemical Reactivity of *N*,*N*,*N′*,*N′*-tetraoctyl diglycolamide (TODGA) with the Dodecane Radical Cation

Gregory P. Horne,[a]*Jacy K. Conrad,[a] Jeffery R. McLachlan,[a,b] Brian M. Rotermund,[c] Andrew R. Cook,[d] Cristian Celis Barros,[c] and Stephen P. Mezyk[e]*

[a] *Center for Radiation Chemistry Research, Idaho National Laboratory, Idaho Falls, ID, P.O. Box 1625, 83415, USA.*

[b] *Department of Chemistry, Florida International University, Miami, Florida 33199, USA.*

[c] *Department of Chemistry and Biochemistry, Florida State University, Tallahassee, Florida 32306, USA.*

[d] *Department of Chemistry, Brookhaven National Laboratory, Upton, New York, 11973, USA.*

[e] *Department of Chemistry and Biochemistry, California State University Long Beach, 1250 Bellflower Boulevard, Long Beach California, 90840-9507, USA.*

*Corresponding authors. E-mail: gregory.horne@inl.gov and stephen.mezyk@csulb.edu.

ORCID

Gregory P. Horne	0000-0003-0596-0660
Jacy K. Conrad	0000-0002-0745-588X
Jeffery R. McLachlan	0000-0001-6944-3377
Brian M. Rotermund	0000-0002-2379-0119
Andrew R. Cook	0000-0001-6633-3447
Cristian Celis Barros	0000-0002-4685-5229
Stephen P. Mezyk	0000-0001-7838-1999

ABSTRACT

The impact of lanthanide (Ln) metal ion complexation and temperature on the chemical reactivity of *N*,*N*,*N′*,*N′*-tetraoctyl diglycolamide (TODGA) with the dodecane radical cation ($RH^{\bullet+}$) has been measured by electron pulse radiolysis and evaluated by quantum mechanical calculations. Additionally, Arrhenius parameters—specifically activation energies (E_a) and pre-exponential factors (A)—were determined for the reaction of the "free" TODGA ligand with the $RH^{\bullet+}$ radical cation from 282-314 K, giving: E_a(TODGA) = 17.43 ± 1.64 kJ mol^{-1}, and A(TODGA) = $(2.36 \pm 0.05) \times 10^{13}$ M^{-1} s^{-1}.The complexation of trivalent neodymium (Nd(III)), gadolinium (Gd(III)), and ytterbium (Yb(III)) by TODGA yielded $[Ln(TODGA)_3(NO_3)_3]$ complexes that exhibited significantly increased reactivity (up to 9.3×) with the $RH^{\bullet+}$ radical cation, relative to the "free" ligand: $k([Ln(TODGA)_3(NO_3)_3] + RH^{\bullet+}) = (8.99 \pm 0.93) \times 10^{10}$, $(2.88 \pm 0.40) \times 10^{10}$, and $(1.53 \pm 0.34) \times 10^{10}$ M^{-1} s^{-1}, for Nd(III), Gd(III), and Yb(III), respectively. The kinetic enhancement measured for these complexes exhibited a dependence on atomic number, decreasing as the lanthanide series was traversed. Preliminary reaction free energy calculations indicated that $RH^{\bullet+}$ radical cation initiated electron/hole and proton transfer is more energetically favorable with the

attendant nitrate counter anions (< -2.82 eV) than for complexed TODGA, and likely to decrease in favorability as the charge density of the bound lanthanide ion increases across the series.

This draft manuscript has been prepared in fulfillment of Milestone M4FT-22IN030402024.

INTRODUCTION

Understanding the impact of ionizing radiation on ligands employed for the separation, recovery, and transport of metal ions is of vital importance for the innovation of nuclear fuel cycle technologies and nuclear medicine. In both fields, novel ligands are designed to selectively form complexes with metal ions in specific oxidation states. For example, the ligand *N*,*N*,*N′*,*N′*-tetraoctyl diglycolamide (TODGA) was designed to enable the separation of the trivalent minor actinides (MA) from the trivalent lanthanides (Ln) in used nuclear fuel (UNF) reprocessing raffinates [1-15]. However, in the presence of ionizing radiation fields—for example, those arising from the radioisotopic content of UNF raffinates or from the radioactive decay of theranostic agents—these complexing ligands are subject to radiolysis, leading to their destruction and the formation of potentially detrimental degradation products. Consequently, mastery of the radiation-induced behavior of these molecules is essential for optimizing their effectiveness and longevity, and minimizing the negative impacts of radiolysis.

To this end, there have been extensive studies on the radiation chemistry of ligands, especially those designed for the separation and recovery of elements from UNF [16-31]. However, most contemporary investigations have focused on the radiolytic behavior of the non-complexed—“free”—ligand, despite literature precedence for their metal ion complexes promoting very different chemical behaviors [32-43]. For example, the complexation of trivalent iron ions by ethylenediaminetetraacetic acid (EDTA)—a typical chelation therapy ligand—was found to accelerate the rate of EDTA radiolysis, as the metal ion center provided additional inner/outer sphere reaction pathways for the products of water radiolysis [33-36]. More recently, trivalent neodymium (Nd(III)) and americium (Am(III)) complexation by TODGA in 5% 1-octanol/*n*-dodecane solvent was shown to *reduce* the extent of steady-state TODGA radiolysis and to alter the suite of degradation products, producing species that were less problematic [44]. Unfortunately, our understanding of the fundamental radiation-induced processes responsible for these divergent steady-state observations is limited, and yet it is essential for accurately predicting their behavior under real-world application conditions and to aid the design of new radiation-resistant ligands.

Elucidation of the underpinning mechanistic changes conferred by metal ion complexation necessitates knowledge of their chemical kinetics, as recently demonstrated for the reaction of uranyl (UO_2^{2+}) complexes of *N*,*N*-di-(2-ethylhexyl)butyramide (DEHBA), *N*,*N*-di-2-ethylhexylisobutryamide (DEH*i*BA), and tributylphosphate (TBP) [43] with the dodecane radical cation ($RH^{\bullet+}$)—an important transient species from the radiolysis ($\rightsquigarrow$) of *n*-dodecane (RH) solutions and solvent systems [42,43,45-49]:

$$RH \rightsquigarrow e^-, H^\bullet, RH^{\bullet+}, R^\bullet, \tag{1}$$

$$\text{Ligand} + RH^{\bullet+} \rightarrow [\text{Ligand}]^{\bullet+}/[\text{Ligand}(+H^+)]^+ + RH/R^\bullet. \tag{2}$$

In the case of DEHBA, DEH*i*BA, and TBP, the complexation of UO_2^{2+} by DEHBA/DEH*i*BA afforded a 2.6×/1.4× faster rate coefficient (k) for the reaction of the $RH^{\bullet+}$ radical cation with the corresponding complexes—$[UO_2(DEHBA)_2(NO_3)_2]$/$[UO_2(DEHiBA)_2(NO_3)_2]$—relative to the free ligands. In contrast, the complementary TBP complex—$[UO_2(TBP)_2(NO_3)_2]$—showed no change in reaction kinetics relative to free TBP [43]. These changes in the chemical reactivity of the ligand complexes were attributed to a combination of differences in reaction pathways (electron/hole transfer *vs*. proton transfer), energetics, and electron density distribution changes upon complexation [43]. Overall, these absolute kinetic measurements provided greater insight into the impact of metal loading on the chemical reactivity of these ligands in radiation environments.

However, to date, no such chemical kinetics knowledge exists for the metal ion complexes of TODGA, despite this ligand exhibiting significantly different radiolytic behavior in the presence of its MA and Ln complexes at steady-state timescales [44]. To bridge this knowledge gap, here we report kinetic measurements demonstrating the impact of selected Ln(III) complexation on the reaction kinetics of the $RH^{\bullet+}$ radical cation with TODGA at ambient temperature (~ 23 ^{o}C). Further, as the real-world application of TODGA in UNF reprocessing systems is expected to operate at temperatures above ambient (> 30 ^{o}C), Arrhenius parameters—notably activation energies (E_a) and pre-exponential factors (A)—were also determined for the reaction of the $RH^{\bullet+}$ radical cation with the free TODGA ligand. These kinetic data are necessary to facilitate the development of computer models to determine predicted longevity under process conditions.

METHODS

Chemicals

N,N,N’,N’-tetraoctyldiglycolamide (TODGA, 99%) was supplied by Eichrom (Lisle, Illinois, USA) and Technocomm Ltd (Wellbrae, Scotland, UK), respectively. Dichloromethane (DCM, ≥ 99.8%), *n*-dodecane (≥ 99% anhydrous), nitric acid (HNO_3, ≥ 99.999% trace metals basis), perchloric acid ($HClO_4$, ≥ 99.999% trace metals basis), and potassium thiocyanate (KSCN, ≥ 99.0% ACS Reagent Grade) were obtained from MilliporeSigma (Burlington, Massachusetts, USA). Nitrate salts of gadolinium (Gd(III), 99.9%), neodymium (Nd(III), 99.99%), and ytterbium (Yb(III), 99.9%), were sourced from Alfa Aesar. All chemicals were used without further purification. Ultra-pure water (18.2 MΩ cm) was used to prepare all aqueous solutions.

Sample Preparation

Free 100 mM TODGA ligand solutions were prepared by weighing the ligand and then directly dissolving it in 0.5 M DCM/*n*-dodecane stock solution. A portion of this free ligand stock solution was used for non-ambient temperature runs, following serial dilution using additional 0.5 M DCM/*n*-dodecane solution. The corresponding lanthanide ion complex solutions were then prepared by pre-equilibrating the free TODGA ligand solution thrice with 1.0 M HNO_3 [50], and then contacting this solution in a 1:1 organic:aqueous ratio, with an aqueous phase comprised of a given lanthanide (~20 mM of either Nd(III), Gd(III), or Yb(III)) in an equivalent volume of 1.0 M HNO_3 solution. For each contact (pre-equilibration and lanthanide extraction), phases were rapidly vortex mixed for 5 minutes, and then the organic phase separated by centrifuge at 4000 rpm for 5 minutes using a Thermo Scientific (Waltham, Massachusetts, USA) Sorvall Legend Centrifuge. The lanthanide loaded organic phases were then used to prepare samples for irradiation by serial dilution with additional pre-equilibrated 0.5 M DCM/*n*-dodecane solution, maintaining a constant TODGA:Ln ratio. The initial and post contact aqueous phases were retained for Inductively-Coupled Plasma Mass Spectrometry (ICP-MS) analyses to quantitatively determine the amount of each lanthanide extracted.

Time-Resolved Electron Pulse Irradiations

Kinetics for reaction of the $RH^{\bullet+}$ radical cation with TODGA in the absence and presence of three representative lanthanide metal ions (Nd(III), Gd(III), and Yb(III)) in 0.5 M DCM/*n*-

dodecane solutions at ambient temperature were measured using the Brookhaven National Laboratory (BNL) Laser Electron Accelerator Facility (LEAF) [51]. Aerated sealed samples were irradiated in static 1.00 cm Suprasil Starna Scientific Ltd. (Ilford, United Kingdom) cuvettes sealed with Teflon stoppers. Dosimetry was determined using N_2O-saturated solutions of 10 mM KSCN at $\lambda_{max} = 470$ nm ($G^*\varepsilon = 5.2 \times 10^{-4}$ m^2 J^{-1}) [52].

The time-resolved changes in the absorption decays of the $RH^{\bullet+}$ radical cation were followed at 800 nm using an FND-100 silicon diode detector, and subsequently digitized using a LeCroy WaveRunner 640Zi oscilloscope (4 GHz, 8 bit). Interference filters (ca. 10 nm bandpass) were used for wavelength selection of the analyzing light. These measured $RH^{\bullet+}$ radical cation decays were fitted using a double-exponential decay function:

$$k_{obs} = \mathrm{A}_1 exp^{-k_1 t} + \mathrm{A}_2 exp^{-k_2 t} + \mathrm{B}, \quad (3)$$

where k_{obs} was the overall rate of decay for the 800 nm $RH^{\bullet+}$ radical cation signal, A_i are the optical density amplitudes, k_i are the pseudo-first-order rate coefficients (s^{-1}), t is time (s), and B is a baseline offset correction. The first exponential decay (A_1 and k_1 parameters) corresponds to the total reaction of the $RH^{\bullet+}$ radical cation with both the free TODGA ligand and the $[Ln(TODGA)_3(NO_3)_3]$ complex,

$$k_1 = ([\mathrm{TODGA}] \times k_{\mathrm{TODGA}}) + ([\mathrm{Complex}] \times k_{\mathrm{Complex}}). \quad (4)$$

while the second exponential decay (A_2 and k_2) and B variables account for the slow tailing decrease seen in these systems [43].

The contribution of the free TODGA ligand reactivity (k_{TODGA}) was calculated based on its measured rate coefficient [45], and its concentration, assuming a constant 3:1 TODGA:Ln ratio complex was formed under our conditions [50,53]. Subtracting this component from the overall fitted k_1 value, and then plotting the difference as a function of solute concentration, gave the final second-order rate coefficient (k_{Complex}) values reported by this work.

Arrhenius parameters were also determined for TODGA in the absence of lanthanide ion complexation, wherein kinetics were measured at several temperatures (282-314 K), allowing for calculation of the reaction's activation energy, E_a (kJ mol^{-1}), and pre-exponential factor, A (M^{-1} s^{-1}) values, using:

$$k = Ae^{\frac{-E_a}{RT}}, \tag{5}$$

where k is the second-order rate coefficient, R is the molar gas constant (J mol^{-1} K^{-1}), and T is the absolute temperature in Kelvin (K).

The quoted rate coefficient and Arrhenius parameter errors (1σ) are a quantitative combination of measurement precision (~4%) and sample concentration (initial concentration (~8%) and dilution (<1%)) errors.

Inductively-Coupled Plasma Mass Spectrometry Metal Ion Analysis

Quantification of the amount of lanthanide metal ion extracted into the organic phases was achieved by ICP-MS. Pre- and post-contact lanthanide aqueous samples were digested entirely in 2% Optima grade HNO_3 and diluted, typically 100-500×. Samples were run on an Agilent (Santa Clara, CA, USA) 7500ce ICP-MS using a helium reaction cell to reduce isobaric interferences. Lanthanide standard solutions were sourced from Inorganic Ventures CMS-1, instrument calibrations used SPEX CertifPrep CL-CAL-2 ICP-MS calibration standards, and the internal standard sample was 20 ppb rhodium from SPEX CertifPrep PLRH2-2Y. Lanthanide and external standards were run at the beginning and end of each sample set measurement. All measurements were performed in triplicate and are summarized in **Table 1**.

Table 1. Results from ICP-MS analysis of the lanthanide/1.0 M HNO_3 aqueous phases pre- and post-contact with pre-equilibrated TODGA/0.5 M DCM/*n*-dodecane organic solution.

Lanthanide	**[Aqueous]$_{\text{Pre}}$** (mM)	**[Aqueous]$_{\text{Post}}$** (mM)	**Δ[Aqueous]** (mM)
Nd(III)	19.49	7.48	12.01
Gd(III)	21.18	1.75	19.43
Yb(III)	20.00	0.38	19.62

Computations

Quantification of electronic structure computations for free TODGA and $[Ln(TODGA)]^{3+}$ in *n*-dodecane solvent used the Gaussian16 and Gaussview6 programs [54,55]. All geometries were determined using density functional theory (DFT) with the B3LYP functional and 6-31+g* basis set. Solvation was included in all calculations using the polarizable continuum model for *n*-dodecane. Reaction free energies for electron/hole *vs*. proton transfer from the $RH^{\bullet+}$ radical cation to TODGA, $[Ln(TODGA)]^{3+}$, HNO_3, and NO_3^- were determined using corrections for standard entropic states [56,57].

RESULTS AND DISCUSSION

The reaction of the $RH^{\bullet+}$ radical cation with the free TODGA ligand can proceed by either electron/hole or proton transfer:

$$\mathrm{TODGA} + \mathrm{RH}^{\bullet+}$$

$$\rightarrow \mathrm{TODGA}^{\bullet+} + \mathrm{RH} \qquad \text{(electron/hole transfer)}, \qquad (6)$$

$$\rightarrow \mathrm{TODGA}(+\mathrm{H}^+) + \mathrm{R}^\bullet \qquad \text{(proton transfer)}, \qquad (7)$$

of which the calculated reaction free energies (ΔG, eV) for these reaction pathways are -1.19 and -1.38 eV, respectively. As both pathways are energetically favorable in *n*-dodecane solvent, albeit with an energetic preference for proton transfer (0.19 eV), we anticipate that lanthanide complexation will alter the kinetic preference for these pathways, thereby influencing the rate of ligand radiolysis and the suite of associated degradation products, as demonstrated for the steady-state radiolysis of TODGA [44].

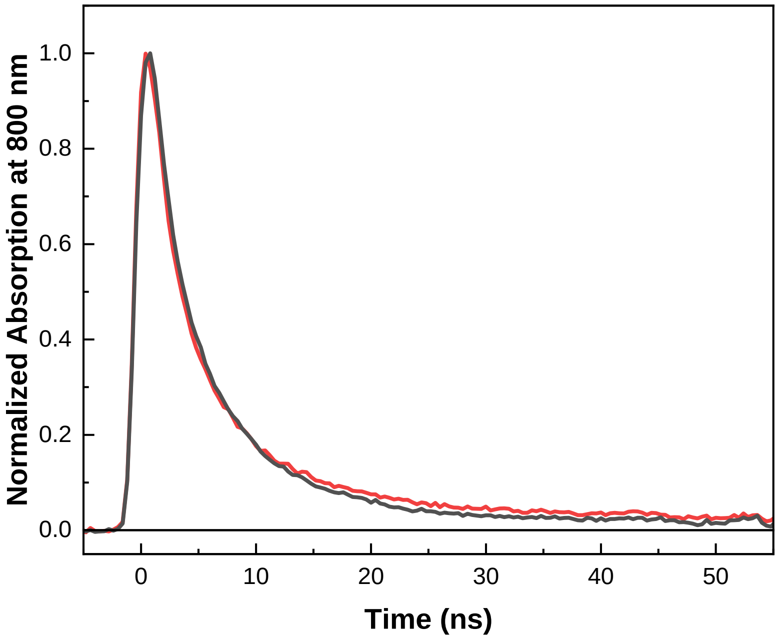

Figure 1. Normalized kinetic traces at 800 nm for electron pulse irradiated solutions of aerated 0.5 M DCM/*n*-dodecane with (**grey**) and without (**red**) pre-equilibration with 1.0 M HNO_3 at ambient temperature.

Prior to TODGA reactivity measurements in *n*-dodecane, the impact of extracted HNO_3 on the decay of the $RH^{•+}$ radical cation was investigated, by irradiating 0.5 M DCM/*n*-dodecane solutions with and without 1.0 M HNO_3 pre-equilibration. Typical data are shown in **Figure 1** for the pre-equilibration with. We found a negligible effect of pre-equilibration on the lifetime of the $RH^{•+}$ radical cation, which is consistent with our calculated reaction free energies for electron/hole (+2.24 eV) and proton (+1.56 eV) transfer between the $RH^{•+}$ radical cation and HNO_3:

$$HNO_3 + RH^{•+} \rightarrow HNO_3^{•+} + RH, \quad (8)$$

$$\rightarrow H_2NO_3^{+} + R^{•}. \quad (9)$$

Both reaction pathways are energetically unfavorable in *n*-dodecane. Therefore, the following observed changes in kinetic behavior are attributed directly to the reaction of the free TODGA ligand and its $[Ln(TODGA)_3(NO_3)_3]$ complexes with the $RH^{•+}$ radical cation.

The measured absolute second-order rate coefficients for the reaction of the $RH^{•+}$ radical cation with TODGA in the absence and presence of complexed lanthanides—Nd(III), Gd(III) and Yb,(III)—are summarized in **Table 2**. For the investigated TODGA and lanthanide concentration ranges, we assumed a constant TODGA:Ln ratio of 3:1 [50], with all the $[Ln(TODGA)_3(NO_3)_3]$ complex rate coefficients given in **Table 2** calculated based on this ratio.

Table 2. Summary of second-order rate coefficients determined by this work at ambient temperature for the reaction of the $RH^{•+}$ radical cation with TODGA in the absence and presence of complexed lanthanides—Nd(III), Gd(III) and Yb(III)—in aerated 0.5 M DCM/*n*-dodecane solutions.

Ligand	**Second-Order Rate Coefficient (k, × 10^{10} M^{-1} s^{-1})**			
	Free Ligand	*Nd(III) Complex*	*Gd(III) Complex*	*Yb(III) Complex*
TODGA	0.97 ± 0.60 [45]	8.99 ± 0.93	2.88 ± 0.40	1.53 ± 0.34

Increasing the concentration of $[Ln(TODGA)_3(NO_3)_3]$ complexes in solution afforded a faster decay of the $RH^{•+}$ radical cation absorption at 800 nm, as demonstrated by the kinetic data shown in **Figure 2** for the $[Nd(TODGA)_3(NO_3)_3]$ complex. Complementary Gd(III) and Yb(III) data are shown the *Supplementary Information*, **Figures S1** and **S2**, respectively. Fitting these decays ultimately gave the second-order rate coefficients given in **Table 2**, all of which are faster than the value for the free ligand (up to 9.3×) [45].

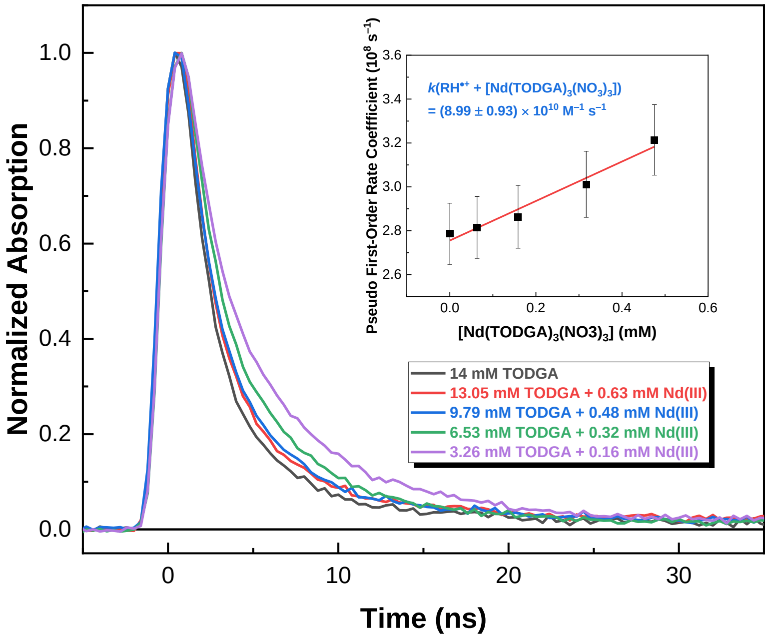

Figure 2. Normalized kinetic traces at 800 nm for electron pulse irradiated solutions of TODGA in the presence and absence of Nd(III) in aerated 0.5 M DCM/*n*-dodecane at ambient temperature: 0 (**grey**), 0.63 (**red**), 0.48 (**blue**), 0.32 (**green**), and 0.16 (**purple**) mM Nd(III). *Inset:* Second-order determination of the rate coefficient for the reaction of [Nd(TODGA)$_3$(NO$_3$)$_3$] with RH$^{•+}$. Individual data points are the faster pseudo-first-order component of the double-exponential fit to the data in the main figure. The weighted linear fit corresponds to a reaction rate coefficient of k([Nd(TODGA)$_3$(NO$_3$)$_3$] + RH$^{•+}$) = $(8.99 \pm 0.93) \times 10^{10}$ M^{-1} s^{-1}.

From a chemical kinetics perspective, the greater reactivity of the [Ln(TODGA)$_3$(NO$_3$)$_3$] complexes, relative to the free ligand, is expected to lead to a faster rate of TODGA radiolysis. However, Kimberlin *et al.* showed that the steady-state gamma irradiation of europium and americium complexes of TODGA reduced the rate of TODGA radiolysis and altered the suite of degradation products, relative to the free TODGA ligand [44]. This suggests that the product(s)—[Ln(TODGA)$_2$(TODGA$^•$)(NO$_3$)$_3$]$^+$ and/or [Ln(TODGA)$_2$(TODGA(+H$^+$))(NO$_3$)$_3$]$^+$—from the reaction of the RH$^{•+}$ radical cation with the [Ln(TODGA)$_3$(NO$_3$)$_3$] complex:

$$[\mathrm{Ln(TODGA)_3(NO_3)_3}] + \mathrm{RH}^{\bullet+}$$

$$\rightarrow [\mathrm{Ln(TODGA)_2(TODGA^{\bullet})(NO_3)_3}]^+ + \mathrm{RH}, \qquad (10)$$

$$\rightarrow [\mathrm{Ln(TODGA)_2(TODGA(+H^+))(NO_3)_3}]^+ + \mathrm{R}^{\bullet}, \qquad (11)$$

is less susceptible to fragmentation than the free TODGA ligand itself. If the instigating reaction between TODGA and the RH$^{•+}$ radical cation is electron/hole transfer (**Equation 10**), the radical formed on a coordinated TODGA molecule could undergo subsequent electron transfer with the complexed lanthanide ion, resulting in the regeneration of the TODGA molecule and the formation of a tetravalent lanthanide oxidation state, Ln(IV), which is unlikely given their standard IV/III redox potentials are very high [58]:

$$[\mathrm{Ln(TODGA)_2(TODGA^\bullet)(NO_3)_3}]^+ \rightarrow [\mathrm{Ln(TODGA)_3(NO_3)_3}]^{\bullet +}. \qquad (12)$$

Alternatively, the TODGA radical could oxidize one of the coordinated NO_3^- anions, leading to the formation of the nitrate radical ($NO_3^\bullet$):

$$[\mathrm{Ln(TODGA)_2(TODGA^\bullet)(NO_3)_3}]^+ \rightarrow [\mathrm{Ln(TODGA)_3(NO_3)_2(NO_3^\bullet)}]^{+}. \qquad (13)$$

Either reaction pathway results in a potent oxidant, Ln(IV) or $NO_3^\bullet$, and yet the "desired" product must be less reactive than the instigating TODGA radical to agree with the observations of Kimberlin *et al.* [44], assuming reaction with the $RH^{\bullet+}$ radical cation is the predominant radiation-induced driving force. In contrast, if the instigating reaction between TODGA and the $RH^{\bullet+}$ radical cation is proton transfer (**Equation 11**), then formation of the $[\mathrm{Ln(TODGA)_2(TODGA(+H^+))(NO_3)_3}]^+$ transient would occur, which could subsequently undergo proton transfer to another species (M) in solution:

$$[\mathrm{Ln(TODGA)_2(TODGA(+H^+))(NO_3)_3}]^+ + \mathrm{M} \rightarrow [\mathrm{Ln(TODGA)_3(NO_3)_3}] + \mathrm{HM}^+, \qquad (14)$$

thereby regenerating the original metal ion-complexed species.

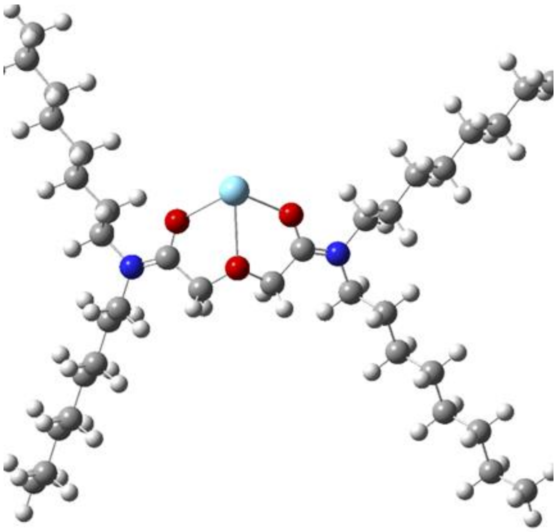

Figure 3. Calculated structure for a single TODGA molecule bound to a Ln(III) center with no NO_3^- counter anions, $[\mathrm{Ln(TODGA)}]^{3+}$.

However, preliminary calculations—based on model system consisting of a single TODGA molecule bound to a Ln(III) center with no counter anions, $[Ln(TOGDA)]^{3+}$, as shown in **Figure 3**—indicate that both reactions become energetically unfavorable upon complexation, +1.64 and +4.85 eV for **Equations 10** and **11**, respectively. In the case of electron/hole transfer, the TODGA radical "hole" resides on one of the octyl chains, and not on the core of the ligand, like it does in free TODGA. The octyl chains have a higher ionization potential (9.80 eV [59]) than *n*-dodecane (< 9.56 eV [60,61]), likely affording the uphill reaction energy calculated here (+1.64 eV). Although more comprehensive $[Ln(TODGA)_3(NO3)_3]$ complex calculations are underway, the free energy values calculated for the $[Ln(TOGDA)]^{3+}$ complex initially suggest that an alternative pathway may be responsible for the kinetic enhancement observed here for the $[Ln(TODGA)_3(NO_3)_3]$ complexes. This alternative mechanism likely involves the attendant NO_3^- counter anions being the target of electron/hole (-3.05 eV) and/or proton (-2.82 eV) transfer with the $RH^{\bullet+}$ radical cation:

$$NO_3^- + RH^{\bullet+}$$

$$\rightarrow NO_3^{\bullet} + RH, \qquad (15)$$

$$\rightarrow HNO_3 + R^{\bullet}, \qquad (16)$$

especially as these pathways are predicted to be more energetically favorable than for the free TODGA ligand and the model $[Ln(TOGDA)]^{3+}$ complex, albeit these values are for non-complexed NO_3^- in *n*-dodecane solvent. This alternative mechanism may also explain the detection of a nitrate-containing TODGA degradation product by Kimberlin *et al.*, which was only seen for TODGA irradiated in the presence of its Nd(III) and Am(III) complexes [44]. However, their Fukui function calculations indicated that the most likely sites for radical attack were on the etheric CH_2 groups on the TODGA backbone in $[Nd(TODGA)_3(NO_3)_3]$/$[Am(TODGA)_3(NO_3)_3]$ complexes. Interestingly, corresponding calculations for coordinated chloride anions (Cl^-)—$[Am(TODGA)_3(Cl)_3]$—predicted preferential reaction at the Cl^- anions. Additionally, our postulation of preferential reaction of the $RH^{\bullet+}$ radical cation with the coordinated NO_3^- anions is consistent with our findings for the complexation of UO_2^{2+} by TBP [43]. Fukui function calculations in that work found that the radical reactivity centers of the $[UO_2(TBP)_2(NO_3)_2]$ complex were on the non-coordinating O-atoms of the coordinated NO_3^- anions, ultimately shielding TBP from reaction with the $RH^{\bullet+}$ radical cation [43]. However, in that scenario, the free TBP ligand was only amenable to proton transfer (-0.36 eV), whereas both electron/hole and proton transfer TODGA, -1.19 and -1.38 eV, respectively. Needless to say, additional quantum mechanical calculations are necessary to resolve the various postulated reaction pathways for $[Ln(TODGA)_3(NO_3)_3]$ complexes.

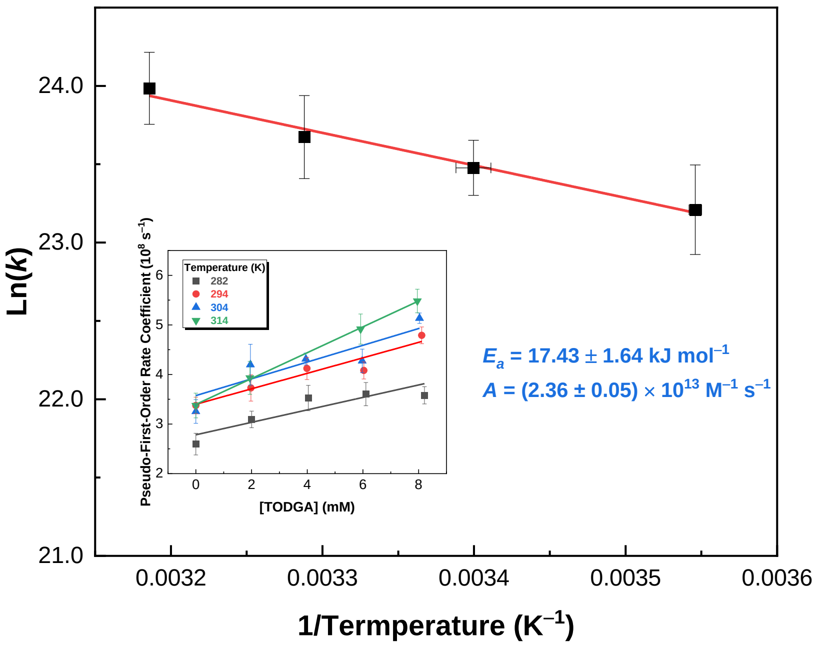

Figure 4. Arrhenius plot for the reaction of TODGA with the $RH^{\bullet+}$ radical cation, affording an $E_a = 17.43 \pm 1.64$ kJ mol^{-1}, and an $A = (2.36 \pm 0.05) \times 10^{13}$ M^{-1} s^{-1}. Individual data points were derived from second-order rate coefficients determined at different temperatures: 282 (■), 294 (●), 304 (▲), and 314 (▼) K, shown in the *Inset*.

Interestingly, the rate coefficient values for the reaction of the $RH^{\bullet+}$ radical cation with the various $[Ln(TODGA)_3(NO_3)_3]$ complexes in **Table 2** decreased with the atomic number of the lanthanide ion: Nd(III) $k = (2.65 \pm 0.60) \times 10^{10}$ < Gd(III) $k = (3.09 \pm 0.44) \times 10^{10}$ < Yb(III) $k = (4.11 \pm 0.49) \times 10^{10}$ M^{-1} s^{-1}. This indicates that the observed kinetic enhancement upon metal ion complexation is the result of a combination of factors, including the relative size of the complex and changes in electron distribution, both of which are influenced by the atomic properties of the complexed metal ion center. With regards to complex size, in going from the free TODGA ligand to the larger $[Ln(TODGA)_3(NO_3)_3]$ complexes, we should expect an increase in the reaction rate. However, as the lanthanide series is traversed—in going from Nd(III) to Gd(III) to Yb(III)—there is a significant contraction in the metal ion ionic radii (1.163, 1.107, and 1.042 Å, respectively, for a 9-coordinate geometry [62]), which would suggest a shrinking in size of the corresponding $[Ln(TODGA)_3(NO_3)_3]$ complexes. This should give a concomitant decrease in chemical reactivity, which is what was observed here (**Table 2**). However, as alluded to above, this is likely only part of the explanation for the change in kinetics with atomic number. This observation could also support radical reaction at the coordinated NO_3^- anions, as **Equations 15** and **16** are expected to be less favorable the more tightly they are associated with the Ln(III) ion, which is expected to occur based on changes in charge density as the lanthanide period is traversed. Both postulations are currently being evaluated by complimentary quantum mechanical calculations [43].

The temperature dependence of the $RH^{\bullet+}$ radical cation reaction with the free TODGA ligand, along with the derived Arrhenius parameters are shown in **Figure 4**. For all investigated temperatures (282-314 K), the rate of reaction increased. The transformed Arrhenius plot gave values of the activation energy, $E_a = 17.43 \pm 1.64$ kJ mol^{-1}, and the pre-exponential factor, $A = (2.36 \pm 0.05) \times 10^{13}$ m^{-1} s^{-1}. The E_a value is consistent with previous values for electrono abstraction radical reactions in water [63], but no comparative kinetic data have been reported in *n*-dodecane. Concomitant experiments for the $[Ln(TODGA)_3(NO_3)_3]$ complexes were not possible due to limitations in instrument time resolution.

CONCLUSIONS

Lanthanide ion complexation by TODGA afforded complexes with increased chemical reactivity (up to 9.3×) towards the $RH^{\bullet+}$ radical cation formed in *n*-dodecane radiolysis. Further, the $[Ln(TODGA)_3(NO_3)_3]$ complexes exhibited reaction rates that decreased as the lanthanide series was traversed—Nd(III) to Gd(III) to Yb(III)—indicating a change in reaction mechanism upon complexation.

Preliminary free energy calculations showed that electron and proton transfer with the $RH^{\bullet+}$ radical cation were both energetically favorable for free TODGA (-1.19 and -1.38 eV, respectively), but highly uphill for the model $[Ln(TOGDA)]^{3+}$ complex (+1.64 and +4.85 eV, respectively) in *n*-dodecane solvent. Consequently, while enhanced reaction rates appeared to implicate differences due to the relative size of the complexes and changes in TODGA ligand and lanthanide electron distributions, one must also consider the impact of the attendant NO_3^- counter anions. The reactions of these anions with the $RH^{\bullet+}$ radical cation are predicted to be highly energetically favorable (< -2.82 eV), and likely also influenced by the charge density of the bound Ln(III) ion, thereby also providing an explanation for the periodicity effect. Consequently, it is possible that reaction with the NO_3^- counter anions dominate the differences in rates we see with the [Ln(TODGA)$_3$(NO$_3$)$_3$] complexes. However, we cannot resolve these potential pathways at this time, although, more comprehensive quantum mechanical calculations are underway to evaluate the energetic feasibility of each pathway.

This draft manuscript has been prepared in fulfillment of Milestone M4FT-22IN030402024.

CONFLICTS OF INTEREST

There are no conflicts to declare.

ASSOCIATED CONTENT

Supplementary Information for "*Additional TODGA-Lanthanide Reaction Kinetic Data*."

AUTHOR INFORMATION

Corresponding Authors

Gregory P. Horne – Center for Radiation Chemistry Research, Idaho National Laboratory, 1955 N. Freemont Ave., Idaho Falls, 83415, USA; orcid.org/0000-0003-0596-0660; E-mail: gregory.horne@inl.gov.

Stephen P. Mezyk – Department of Chemistry and Biochemistry, California State University Long Beach, 1250 Bellflower Boulevard, Long Beach California, 90840-9507, USA.; orcid.org/0000-0001-7838-1999; E-mail: stephen.mezyk@csulb.edu.

ACKNOWLEDGEMENTS

This research has been funded by the U.S. Department of Energy Assistant Secretary for Nuclear Energy, under the Material Recovery and Waste Form Development Campaign, DOE-Idaho Operations Office Contract DE-AC07-05ID14517.

REFERENCES

(1) Y. I. Sasaki and G.R. Choppin, Solvent extraction of Eu, Th, U, Np and Am with N,N'-dimethyl-N,N'-dihexyl-3-oxapentanediamide and its analogous compounds. *Anal. Sci.*, **1996**, *12*, 225–230.

(2) Y. Sasaki and G.R. Choppin, Extraction of Np(V) by N,N'-dimethyl-N,N'-dihexyl-3-oxapentanediamide. *Radiochim. Acta*, **1998**, *80*, 85–88.

(3) Y. Sasaki, Y. Sugo, S. Suzuki, and S. Tachimori, The novel extractants, diglycolamides, for the extraction of lanthanides and actinides in HNO_3-*n*-dodecane system. *Solvent Extr. Ion Exch.*, **2001**, *19* , 91–103.

(4) S. Tachimori, Y. Sasaki, and S. Suzuki, Modification of TODGA-n-dodecane solvent with a monoamide for high loading of lanthanides(III) and actinides(III). *Solvent Extr. Ion Exch.*, **2002**, *20*, 687–699.

(5) A. Geist, U. Mullich, D. Magnusson, P. Kaden, G. Modolo, A. Wilden, and T. Zevaco, Actinide(III)/Lanthanide(III) Separation Via Selective Aqueous Complexation of Actinides(III) using a Hydrophilic 2,6-Bis(1,2,4-Triazin-3-Yl)-Pyridine in Nitric Acid. *Solvent Extr. Ion Exch.*, **2012**, *30*, 433–444.

(6) K. Bell, C. Carpentier, M. Carrott, A. Geist, C. Gregson, X. Heres, D. Magnusson, R. Malmbeck, F. McLachlan, G. Modolo, U. Mullich, M. Sypula, R. Taylor, and A. Wilden, Progress towards the development of a new GANEX process. *Procedia Chem.*, **2012**, *7*, 392–397.

(7) J. Brown, F. McLachlan, M. Sarsfield, R. Taylor, G. Modolo, and A. Wilden, Plutonium Loading of Prospective Grouped Actinide Extraction (GANEX) Solvent Systems based on Diglycolamide Extractants. *Solvent Extr. Ion Exch.*, **2012**, 30, 127–141.

(8) S.A. Ansari, P. Pathak, P.K. Mohapatra, and V.K. Manchanda, Chemistry of Diglycolamides: Promising Extractants for Actinide Partitioning. *Chem. Rev.*, **2012**, *112*, 1751–1772.

(9) M.J. Carrot, C.R. Gregson, and R.J. Taylor, Neptunium Extraction and Stability in the GANEX Solvent: 0.2 M TODGA/0.5 M DMDOHEMA/Kerosene. *Solvent Extr. Ion Exch.*, **2013**, 31, 463–482.

(10) G. Modolo, A. Wilden, P. Kaufholz, D. Bosbach, and A. Geist, Development and demonstration of innovative partitioning processes (i-SANEX and 1-cycle SANEX) for actinide partitioning. *Prog. Nucl. Energy*, **2014**, *72*, 107–114.

(11) A. Wilden, G. Modolo, P. Kaufholz, F. Sadowski, S. Lange, M. Sypula, D. Magnusson, U. Mullich, A. Geist, and D. Bosbach, Laboratory-Scale Counter-Current Centrifugal Contactor Demonstration of an Innovative-SANEX Process Using a Water Soluble BTP. *Solvent Extr. Ion Exch.*, **2015**, *33*, 91–108.

(12) M. Carrott, A. Geist, X. Hères, S. Lange, R. Malmbeck, M. Miguirditchian, G. Modolo, A. Wilden, and R. Taylor, Distribution of plutonium, americium and interfering fission products between nitric acid and a mixed organic phase of TODGA and DMDOHEMA in kerosene, and implications for the design of the "EURO-GANEX" process. *Hydrometallurgy*, **2015**, *152*, 139–148.

(13) D. Whittaker, A. Geist, G. Modolo, R. Taylor, M. Sarsfield, and A. Wilden, Applications of Diglycolamide Based Solvent Extraction Processes in Spent Nuclear Fuel Reprocessing, Part 1: TODGA. *Solvent Extr. Ion Exch.*, **2018**, *36*, 223–256.

(14) R. Malmbeck, D. Magnusson, S. Bourg, M. Carrott, A. Geist, X. Heres, M. Miguirditchian, G. Modolo, U. Mullich, C. Sorel, R. Taylor, and A. Wilden, Homogenous recycling of transuranium elements from irradiated fast reactor fuel by the EURO-GANEX solvent extraction process. *Radiochim. Acta*, **2019**, *107*, 917–929.

(15) C. Marie, P. Kaufholz, V. Vanel, M.-T. Duchesne, E. Russello, F. Faroldi, L. Baldini, A. Casnati, A. Wilden, G. Modolo, and M. Miguirditchian, Development of a Selective Americium Separation Process Using H4TPAEN as Water-Soluble Stripping Agent*Solvent Extr. Ion Exch.*, **2019**, *37*, 313–327.

(16) B.J. Mincher and S.P. Mezyk, Radiation Chemical Effects on Radiochemistry: A Review of Examples Important to Nuclear Power. *Radiochim. Acta*, **2009**, *97*, 519–534.

(17) B.J. Mincher, G. Modolo, and S.P. Mezyk, Review Article: The Effects of Radiation Chemistry on Solvent Extraction: 1. Conditions in Acidic Solution and a Review of TBP Radiolysis. *Solv. Extr. Ion Exch.*, **2009a**, *27 (1)*, 1–25.

(18) B.J. Mincher, G. Modolo, and S.P. Mezyk, Review Article: The Effects of Radiation Chemistry on Solvent Extraction: 2. A Review of Fission-Product Extraction. *Solv. Extr. Ion Exch.*, **2009b**, *27 (3)*, 331–353.

(19) B.J. Mincher, G. Modolo, and S.P. Mezyk, Review Article: The Effects of Radiation Chemistry on Solvent Extraction 3: A Review of Actinide and Lanthanide Extraction. *Solv. Extr. Ion Exch.* **2009c**, *27 (5–6)*, 579–606.

(20) L. Berthon and M.-C. Charbonnel, Chapter 8 Radiolysis of Solvents Used in Nuclear Fuel Reprocessing, Ion Exchange and Solvent Extraction: A Series of Advances, Volume 19, B.A. Moyer (Editor), 429–514.

(21) R. Malmbeck and N. L. Banik, Radiolytic behavior of a TODGA based solvent under alpha irradiation. *J. Radioanal. Nucl. Chem.*, **2020**, *326*, 1609–1615.

(22) H. Galan, C.A. Zarzana, A. Wilden, A. Nunez, H. Schmidt, R.J.M. Egberink, A. Leoncini , J. Cobos , W. Verboom , G. Modolo , G. S. Groenewold and B. J. Mincher , Gamma-radiolytic stability of new methylated TODGA derivatives for minor actinide recycling. *Dalton Trans.*, **2015**, *44*, 18049–18056.

(23) V. Hubscher-Bruder, V. Mogilireddy, S. Michel, A. Leoncini, J. Huskens, W. Verboom, H. Galan, A. Nunez, J. Cobos, G. Modolo, A. Wilden, H. Schmidt, M.C. Charbonnel, P. Guilbaud, and N. Boubals, Behaviour of the extractant Me-TODGA upon gamma irradiation: quantification of degradation compounds and individual influences on complexation and extraction. *New J. Chem.*, **2017**, *41*, 13700–13711.

(24) H. Galan, A. Nunez, A.G. Espartero, R. Sedano, A. Durana, and J. de Mendoza, Radiolytic stability of TODGA: Characterization of degraded samples under different experimental conditions. *Proc. Chem.*, **2012**, *7*, 195–201.

(25) C.A. Zarzana, G.S. Groenewold, B.J. Mincher, S.P. Mezyk, A. Wilden, H. Schmidt, G. Modolo, J.F. Wishart, and A.R. Cook, A Comparison of the γ-Radiolysis of TODGA and T(EH)DGA Using UHPLC-ESI-MS Analysis. *Solvent Extr. Ion Exch.*, **2015**, *33* , 431–447.

(26) K.M. Roscioli-Johnson, C.A. Zarzana, G.S. Groenewold, B.J. Mincher, A. Wilden, H. Schmidt, G. Modolo, and B. Santiago-Schübel, A Study of the Radiolysis of N,N-Didodecyl-N',N'-Dioctyldiglycolamide Using UHPLC-ESI-MS Analysis. *Solvent Extr. Ion Exch.*, **2016**, *34*, 439–453.

(27) I. Sánchez-García, H. Galán, J.M. Perlado, and J. Cobos, Stability studies of GANEX system under different irradiation conditions. *EPJ Nuclear Sci. Technol.*, **2019**, *5*, 19–26.

(28) I. Sanchez-Garcia, H. Galan, J.M. Perlado, and J. Cobos, Development of experimental irradiation strategies to evaluate the robustness of TODGA and water-soluble BTP extraction systems for advanced nuclear fuel recycling. *Radiat. Phys. Chem.*, **2020**, *177* , 109094.

(29) Y. Wang, Y. Wan, Y. Cai, L. Yuan, W. Feng, and N. Liu, A review of the alpha radiolysis of extractants for actinide lanthanide separation in spent nuclear fuel reprocessing. *Radiochim. Acta*, **2021**, *109*, 603–623.

(30) Y. Sugo , M. Taguchi , Y. Sasaki , K. Hirota and T. Kimura , Radiolysis study of actinide complexing agent by irradiation with helium ion beam. *Radiat. Phys. Chem.*, **2009**, *78*, 1140–1144.

(31) Y. Sugo, Y. Sasaki, M. Taguchi, and N.S. Ishioka, α-Radiation effect on solvent extraction of minor actinide. *J. Radioanal. Nucl. Chem.*, **2015**, *303*, 1381–1384.

(32) G.V. Buxton and R.M. Sellers, The radiation chemistry of metal ions in aqueous solution. *Coord. Chem. Rev.*, **1977**, *22 (3)*, 195–274.

(33) S.N. Bhattacharyya and K.P. Kundu, The radiation chemistry of aqueous solutions of ferric ethylenediamine tetraacetate. *Int. J. Radiat. Phys. Chem.*, **1971**, *3*, 1–10.

(34) K.P. Kundu and N. Matuura, Gamma-radiolysis of ferric ethylene diamine tetra-acetate in neutral aqueous solution. *Int. J. Radiat. Phys. Chem.*, **1975**, *7*, 565–571.

(35) G.R. Buettner, T.P. Doherty, and L.K. Patterson, The kinetics of the reaction of superoxide radical with iron(III) complexes of EDTA, DETAPAC and HEDTA. *FEBS Lett.*, **1983**, *158*, 143–146.

(36) Y.A. Ilan and G. Czapski, The reaction of superoxide radical with iron complexes of EDTA studied by pulse radiolysis. *Biochimica et Biophysica Acta*, **1977**, *498*, 386–394.

(37) B.K. Sharma and R. Gupta, γ-Radiolysis of aqueous solutions of cerium(III)-ethylenediamine tetraacetate. *Radiat. Eff. Lett.*, **1980**, *57*, 149–154.

(38) B.K. Sharma and R. Gupta, On the γ-radiolysis of aqueous solution of cerium(III) nitriloltriacetate *Radiat. Phys. Chem.*, **1984**, *24*, 233–237.

(39) M.M. Khater, I.M. Kenawi, A.M. Atwa, and M. B. Hafez, Radiolysis of NTA complexes with uranium(VI), iron(III) and nickel(II). *J. Radioanal. Nucl. Chem.*, **1987**, *111*, 17–26.

(40) N.E. Bibler, Gamma and alpha radiolysis of aqueous solutions of diethylenetriaminepentaacetic acid. *J. Inorg. Nucl. Chem.*, **1972**, *34*, 1417–1425.

(41) M.B. Hafez, H. Roushdy, and N. Hafez, Radiolysis of aqueous solutions of ethylenediaminetetraacetatocerium(III). *J. Radioanal. Chem.*, 1978, **43** , 121–129.

(42) T. Toigawa, D.R. Peterman, D.S. Meeker, T.S. Grimes, P.R. Zalupski, S.P. Mezyk, A.R. Cook, S. Yamashita, Y. Kumagai, T. Matsumura, and G.P. Horne, Radiation-Induced Effects on the Extraction Properties of Hexa-n-octylnitrilo-triacetamide (HONTA) Complexes of Americium and Europium. *Phys. Chem. Chem. Phys.*, **2021**, *23*, 1343–1351.

(43) C. Celis-Barros, C.D. Pilgrim, A.R. Cook, T.S. Grimes, S.P. Mezyk, and G.P. Horne, Influence of Uranyl Complexation on the Reaction Kinetics of the Dodecane Radical

Cation with Used Nuclear Fuel Extraction Ligands (TBP, DEHBA, and DEHiBA). *Physical Chemistry and Chemical Physics*, **2021**, *23*, 24589–24597.

(44) A. Kimberlin, G. Saint-Louis, D. Guillaumont, B. Camès, P. Guilbaud, and L. Berthon, Effect of metal complexation on diglycolamide radiolysis: a comparison between ex situ gamma and in situ alpha irradiation. *Phys. Chem. Chem. Phys.*, **2022**, *24*, 9213–9228.

(45) C.A. Zarzana, G.S. Groenewold, B.J. Mincher, S.P. Mezyk, A. Wilden, H. Schmidt, G. Modolo, J.F. Wishart, and A.R. Cook, A Comparison of the γ-Radiolysis of TODGA and T(EH)DGA Using UHPLC-ESI-MS Analysis. *Solv. Extr. Ion Exch.*, **2015**, *33 (5)*, 431–447.

(46) S.P. Mezyk, B.J. Mincher, S.B. Dhiman, B. Layne and J.F. Wishart, The role of organic solvent radical cations in separations ligand degradation. *J. Radioanal. Nucl. Chem.*, **2016**, *307 (3)*, 2445–2449.

(47) S.P. Mezyk, G.P. Horne, B.J. Mincher, P.R. Zalupski, A.R. Cook, and J.F. Wishart, The Chemistry of Separations Ligand Degradation by Organic Radical Cations. *Proc. Chem.*, **2016**, *21*, 61–65.

(48) J. Drader, G. Saint-Louis, J.M. Muller, M.-C. Charbonnel, P. Guilbaud, L. Berthon, K.M. Roscioli-Johnson, C.A. Zarzana, C. Rae, G.S. Groenewold, B.J. Mincher, S.P. Mezyk, K. McCann, S.G. Boyes, and J. Braley, Radiation chemistry of the branched-chain monoamide di-2-ethylhexyl-isobutyramide. *Solv. Extr. Ion Exch.*, **2017**, *35 (7)*, 480–495.

(49) G.P. Horne, C.A. Zarzana, T.S. Grimes, C. Rae, J. Ceder, S.P. Mezyk, B.J. Mincher, M.-C. Charbonnel, P. Guilbaud, G. Saint-Louis, and L. Berthon, Effect of chemical environment on the radiation chemistry of N,N-di-(2-ethylhexyl)butyramide (DEHBA) and plutonium retention. *Dalton Trans.*, **2019**, *48*, 14450–14460.

(50) M.P. Jensen, T. Yaita, and R. Chiarizia, Reverse-Micelle Formation in the Partitioning of Trivalent f-Element Cations by Biphasic Systems Containing a Tetraalkyldiglycolamide. *Langmuir*, **2007**, *23 (9)*, 4765–4774.

(51) J.F. Wishart, A.R. Cook, and J.R. Miller, The LEAF picosecond pulse radiolysis facility at Brookhaven National Laboratory. *Rev. Sci. Instr.*, **2004**, *75 (11)*, 4359–4366.

(52) G.V. Buxton and C.R. Stuart, Re-evaluation of the thiocyanate dosimeter for pulse radiolysis. *J. Chem. Soc. Faraday Trans.*, **1995**, *92*, 279–281.

(53) T. Fujii, K. Aoki, and H. Yamana, Effect of Nitric Acid Distribution on Extraction Behavior of Trivalent F-Elements in a TRUEX System. *Solv. Extr. Ion Exch.* **2006**, *24 (3)*, 347–357.

(54) M.J. Frisch, G.W. Trucks, H.B. Schlegel, G.E. Scuseria, M.A. Robb, J.R. Cheeseman, G. Scalmani, V. Barone, G.A. Petersson, H. Nakatsuji, X. Li, M. Caricato, A.V. Marenich, J. Bloino, B.G. Janesko, R. Gomperts, B. Mennucci, H.P. Hratchian, J.V. Ortiz, A.F. Izmaylov, J.L. Sonnenberg, D. Williams-Young, F. Ding, F. Lipparini, F. Egidi, J. Goings, B. Peng, A. Petrone, T. Henderson, D. Ranasinghe, V.G. Zakrzewski, J. Gao, N. Rega, G. Zheng, W. Liang, M. Hada, M. Ehara, K. Toyota, R. Fukuda, J. Hasegawa, M. Ishida, T. Nakajima, Y. Honda, O. Kitao, H. Nakai, T. Vreven, K. Throssell, J.A. Montgomery, J.E. Peralta, F. Ogliaro, M.J. Bearpark, J.J. Heyd, E.N. Brothers, K.N. Kudin, V.N. Staroverov, T.A. Keith, R. Kobayashi, J. Normand, K. Raghavachari, A.P. Rendell, J.C. Burant, S.S.

Iyengar, J. Tomasi, M. Cossi, J.M. Millam, M. Klene, C. Adamo, R. Cammi, J.W. Ochterski, R.L. Martin, K. Morokuma, O. Farkas, J.B. Foresman, and D.J. Fox, Gaussian 16, Revision A.03, Gaussian, Inc., Wallingford CT, **2016**.

(55) R. Dennington, T. Keith, and J. Millam, GaussView, Version 6.1.1, Release notes. Semichem Inc., Shawnee Mission, KS, **2019**.

(56) C.P. Kelly, C.J. Cramer, and D.G. Truhlar, Aqueous Solvation Free Energies of Ions and Ion-Water Clusters Based on an Accurate Value for the Absolute Aqueous Solvation Free Energy of the Proton. *J. Phys. Chem. B*, **2006**, *110 (32)*, 16066–16081.

(57) C.P. Kelly, C.J. Cramer, and D. G. Truhlar, Single-Ion Solvation Free Energies and the Normal Hydrogen Electrode Potential in Methanol, Acetonitrile, and Dimethyl Sulfoxide. *J. Phys. Chem. B*, **2007**, *111 (2)*, 408–422.

(58) A.J. Bard, R. Parsons, and J. Jordan, Standard Potentials in Aqueous Solution, Marcel Dekker Inc., New York, **1985**.

(59) https://webbook.nist.gov/cgi/cbook.cgi?Name=octane&Units=SI&cIE=on, last accessed 09/20/2022.

(60) https://webbook.nist.gov/cgi/cbook.cgi?Name=undecane&Units=SI&cIE=on, last accessed 09/20/2022.

(61) S.G. Lias, "Ionization Energy Evaluation" in NIST Chemistry WebBook, NIST Standard Reference Database Number 69, Eds. P.J. Linstrom and W.G. Mallard, National Institute of Standards and Technology, Gaithersburg MD, 20899.

(62) R.D. Shannon, Revised effective ionic radii and systematic studies of interatomic distances in halides and chalcogenides. *Acta Cryst.*, **1976**, A32, 751–767.

(63) G.V. Buxton, C.L. Greenstock, W.P. Helman, and A.B. Ross, Critical review of rate constants for reactions of hydrated electrons, hydrogen atoms and hydroxyl radicals ($^{\bullet}$OH/$^{\bullet}$O^{-}) in aqueous solution. *J. Phys. Chem. Ref. Data*, **1988**, *17*, 513–886.

Supplementary Information for: Impact of Metal Loading and Temperature on the Chemical Reactivity of *N*,*N*,*N′*,*N′*-tetraoctyl diglycolamide (TODGA) with the Dodecane Radical Cation

Gregory P. Horne, Jacy K. Conrad, Jeffery R. McLachlan, Brian M. Rotermund, Andrew R. Cook, Cristian Celis Barros, and Stephen P. Mezyk

Additional TODGA-Lanthanide Reaction Kinetic Data

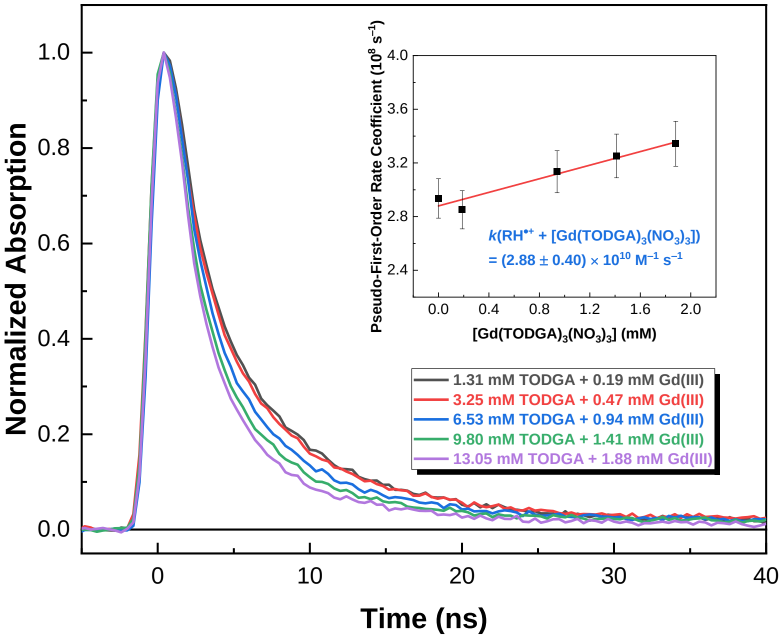

Figure S1. Normalized kinetic traces at 800 nm for electron pulse irradiated solutions of TODGA in the presence and absence of Gd(III) in aerated 0.5 M DCM/*n*-dodecane at ambient temperature: 0.19 (**grey**), 0.47 (**red**), 0.94 (**blue**), 1.41 (**green**), and 1.88 (**purple**) mM Gd(III). *Inset:* Second-order determination of the rate coefficient for the reaction of [Gd(TODGA)$_3$(NO$_3$)$_3$] with RH$^{•+}$ radical cation. Individual data points are the faster pseudo-first-order component of the double-exponential fit to the data shown in the main figure. The weighted linear fit corresponds to a second-order reaction rate coefficient of k([Gd(TODGA)$_3$(NO$_3$)$_3$] + RH$^{•+}$) = (2.88 ± 0.40) × 10^{10} M^{-1} s^{-1}.

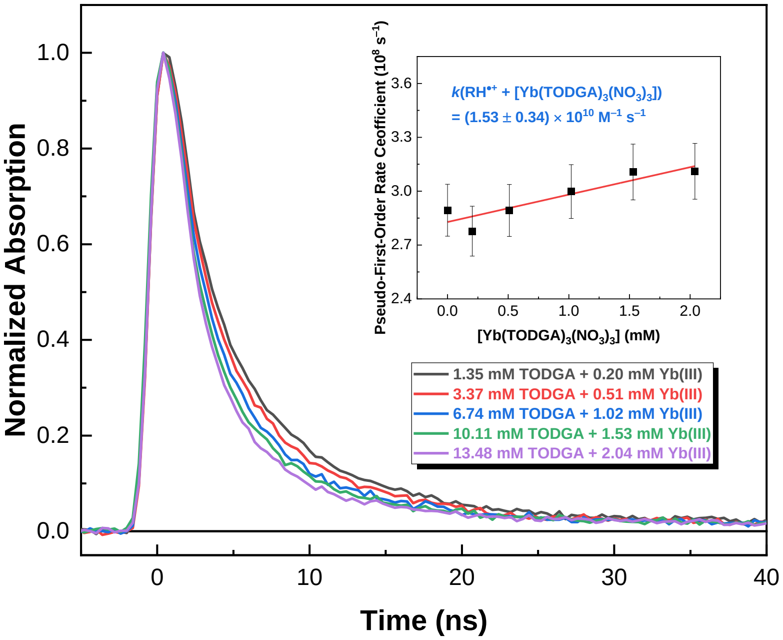

Figure S4. Normalized kinetic traces at 800 nm for electron pulse irradiated solutions of TODGA in the presence and absence of Gd(III) in aerated 0.5 M DCM/*n*-dodecane at ambient temperature: 0.20 (**grey**), 0.51 (**red**), 1.02 (**blue**), 1.53 (**green**), and 2.04 (**purple**) mM Yb(III). *Inset:* Second-order determination of the rate coefficient for the reaction of [Gd(TODGA)$_3$(NO$_3$)$_3$] with RH$^{\bullet+}$ radical cation. Individual data points are the faster pseudo-first-order component of the double-exponential fit to the data shown in the main figure. The weighted linear fit corresponds to a second-order reaction rate coefficient of k([Yb(TODGA)$_3$(NO$_3^-$)$_3$] + RH$^{\bullet+}$) = (1.53 ± 0.34) × 10^{10} M^{-1} s^{-1}.